Fault Detection and Fault-Tolerant Control of a Civil Aircraft Using a Sliding-Mode-Based Scheme

Halim Alwi and Christopher Edwards

***Abstract*—This paper presents a sliding-mode approach for fault-tolerant control of a civil aircraft, where both actuator and sensor faults are considered. For actuator faults, a controller is designed around a state-feedback sliding-mode scheme where the gain of the nonlinear unit vector term is allowed to adaptively increase at the onset of a fault. Unexpected deviation of the switching variables from their nominal condition triggers the adaptation mechanism. The controller proposed here is relatively simple and yet is shown to work across the entire "up and away" flight envelope. For sensor faults, the application of a robust method for fault reconstruction using a sliding-mode observer is considered. The novelty lies in the application of the sensor fault reconstruction scheme to correct the corrupted measured signals before they are used by the controller, and therefore the controller does not need to be reconfigured.**

***Index Terms*—Fault detection and isolation, fault-tolerant control, reconfigurable control, sliding modes.**

I. Introduction

THE safety of aircraft passengers has been and will continue to be an important issue in the commercial aviation industry. All pilots undergo extensive training to help them to be able to react to unforeseen difficulties that may arise during a flight. Additionally, advanced fault-tolerant control systems are designed to help pilots overcome abnormal situations that previously might have resulted in catastrophic events. The increasing importance of fault-tolerant control (FTC) has helped to stimulate a growing body of research work in the area. A recent paper by Zhang and Jiang [24] provides a classification and bibliographical review of FTC in general, especially for so-called "active" FTC [15]. In terms of flight control applications, a survey paper by Huzmezan and Maciejowski [9] describes the latest developments in this subarea. The papers by Hess and Wells [8] and Shtessel *et al.* [16] represent some of the most important recent research in the field of flight control using sliding-mode techniques [20]. The insensitivity and robustness properties of sliding modes to certain types of disturbance and uncertainty [4], [20] make it attractive for applications in the area of flight control and FTC. The work by Hess and Wells [8] argues that sliding-mode control has the potential to become an alternative to reconfigurable control and has the ability to maintain the desired performance without requiring fault detection and isolation (FDI). This represents a so-called "passive" approach to FTC [15]. Alternatively, Shtessel *et al.* [16] use sliding modes with online reconfiguration of the sliding surface boundary layer to control the aircraft in the presence of faults.

Zhang and Jiang [24] argue that, in active FTC systems (AFTCS), good FDI is needed. They claim that, for the system to react properly to a fault, timely and accurate detection and location of the fault is needed. The most researched area in FDI is the residual generation approach using observers—see, for example, Chen and Patton [3]. Observer-based FDI schemes are very dependent on the models about which the scheme is designed. Plant-model mismatches can cause false alarms or—even worse—missed faults. Robustness issues in FDI are therefore very important: for descriptions of the approaches that have been adopted to tackle these issues, see, for example, Chen and Patton [3]. A generic FDI development in terms of reconstruction of faults using sliding mode observers is given by Edwards *et al.* [5] and Tan and Edwards [19]. The novelty of the work done by Edwards *et al.* [5] is the use of the concept of the "equivalent output error injection signal" to reconstruct faults. Tan and Edwards [19] extended this work for robust reconstruction of sensor and actuator faults by minimizing the effect of uncertainty on the reconstruction in an $\mathcal{L}_2$ sense [10].

In this paper, sliding-mode schemes for FTC are developed and applied to an aircraft system. The system is a high-fidelity model of a Boeing 747 which has been used by other researchers as a test bed for their developments: see, for example, [6] and [11]–[14]. The design of the sliding-mode switching surface for the controller uses a new idea building on previous work from the sliding-mode literature [20]. A novel adaptive gain is used in the nonlinear part of the control law which reacts to the occurrence of a fault and attempts to keep the switching function as close as possible to zero, thus trying to maintain nominal tracking performance. If total failure of an actuator is detected, a switch is made to a "back-up" control surface, but the linear component of the control law remains unchanged. This controller is then tested in a number of different actuator fault scenarios. Compared with the work of Hess and Wells [8] and Shtessel *et al.* [16], the novelty of this paper is the design of the sliding hyperplane, which minimizes the effect of unmatched uncertainty on the sliding motion arising from actuator failures, and the development of a simple adaptive scheme for the nonlinear unit vector scaling gain.

A sensor FTC scheme is also proposed in this paper. The novelty lies in the application of a sensor fault reconstruction signal to correct the corrupted measured signals before they are used by the controller, based on a sliding-mode observer. Although the flight condition, faults, and failure tests are similar to those of [6], this paper will show the capabilities of sliding-mode control schemes not only to handle faults, but also failures without

Manuscript received January 20, 2006; revised March 1, 2007. Manuscript received in final form May 23, 2007. Recommended by Associate Editor L. Corradini. This work was supported by the Engineering and Physical Sciences Research Council (EPSRC) under Grant GR/S70876.

The authors are with the Control and Instrumentation Research Group, Department of Engineering, University of Leicester, Leicester LE1 7RH, U.K. (e-mail: ha18@le.ac.uk; chris.edwards@le.ac.uk).

Color versions of one or more of the figures in this paper are available online at http://ieeexplore.ieee.org.

Digital Object Identifier 10.1109/TCST.2007.906311

reconfiguring the overall structure of the controller. The controller is relatively simple but is shown to work across a wide flight envelope without any gain scheduling. Compared with [14], it will be shown that the sliding-mode controller can maintain performance with significant actuator faults without explicitly detecting them.

II. FTLAB747 V6.1/V6.5

Here, we describe the model that will be used as a test bed for the schemes which will be developed in this paper. The FTLAB747 software running under MATLAB has been developed for the study of FTC and FDI schemes. It represents a "real-world" model of a B747-100/200 aircraft, where the technical data and the underlying differential equations have been obtained from NASA [7], [12]. The software was originally initiated at Delft University by van der Linden (Delft University Aircraft Simulation and Analysis Tool, DASMAT) [21] and Smaili (Flight Lab 747, FTLAB747) [17] and later developed and enhanced for use in terms of fault detection and FTC by Marcos and Balas [12] (FTLAB747 V6.1/V6.5). The high-fidelity nonlinear model has 77 states incorporating rigid body variables, sensors, actuators, and aero-engine dynamics. All of the control surfaces and engine dynamics are modeled with realistic position limits and rate limits. The specific aerodynamic coefficients are taken from [7], which have been obtained from extensive wind tunnel experiments, simulations, and test flights. The capabilities of this software as a realistic platform to test FTC and FDI schemes is demonstrated by its subsequent use by many researchers (see, for example, Marcos *et al.* [14], Ganguli *et al.* [6], and Maciejowski and Jones [11]).

In this paper, only longitudinal control is considered: all lateral and directional movement has been set to trim values. This is similar to the scenario considered in [6]. The controller is designed for an "up and away" [6] flight envelope, and the main objective is to obtain good tracking of flight path angle (FPA) and true airspeed (V_{tas}). The nominal (fault-free) sliding-mode controller has first been designed using a linear model obtained from FTLAB747. The linearization has been obtained around an operating condition of 300 000 Kg, 184-m/s true airspeed, and an altitude of 4000 m at half-maximum thrust. The result is a sixth-order model associated with pitch rate q, true airspeed V_{tas}, angle of attack α, pitch angle θ, altitude h_e, and horizontal position along the earth's x-axis x_e. For design purposes, only the first four states have been retained, and the four individual engine thrusts have been aggregated to produce a single control input. The two other inputs represent elevator deflection and horizontal stabilizer deflection. In the following state-space representation, the three inputs have been individually scaled which results in a system and input distribution matrix pair (A_p, B_p) with

$$A_p = \begin{bmatrix} -0.6803 & 0.0002 & -1.0490 & 0 \\ -0.1463 & -0.0062 & -4.6726 & -9.7942 \\ 1.0050 & -0.0006 & -0.5717 & 0 \\ 1 & 0 & 0 & 0 \end{bmatrix}$$

$$B_p = \begin{bmatrix} -1.5539 & 0.0154 \\ 0 & 1.3287 \\ -0.0398 & -0.0007 \\ 0 & 0 \end{bmatrix}$$

$$b_s = \begin{bmatrix} -1.5760 \\ 0 \\ -0.0398 \\ 0 \end{bmatrix} \tag{1}$$

where the states represent pitch rate (radians per second), true airspeed (metres per second), angle of attack (radians), and pitch angle (radians), respectively. The inputs associated with B_p are elevator deflection (radians) and total thrust (Newtons) (scaled by 10^5), and b_s is the distribution matrix associated with the horizontal stabilizer.

During normal operation, the aircraft would be controlled using the thrust and elevator; however, in the event of an elevator failure, the horizontal stabilizer can be used as "backup." In this situation, b_s will be used to replace the first column of B_p when the "backup" controller is activated (this will be discussed later). When implementing the controller on the nonlinear model, a simple gain block (10^5 for thrust and 0.5 for horizontal stabilizer [6]) is used to recover the signal sent to the actuator. The controlled output distribution matrix is

$$C_c = \begin{bmatrix} 0 & 0 & -1 & 1 \\ 0 & 1 & 0 & 0 \end{bmatrix} \tag{2}$$

which represents flight-path angle (FPA) and true airspeed (V_{tas}). This linear model will be used to design the controller and observer schemes which will be described in the following sections.

III. ACTUATOR FTC

This section will concentrate on the design of a fault tolerant controller to handle actuator faults. Consider the nth-order linear time-invariant system with m inputs subject to uncertainty given by

$$\dot{x}_p(t) = A_p x_p(t) + B_p u(t) - B_p K(t) u(t) + M_p \xi(t, x_p) \tag{3}$$

where $A_p \in \mathbb{R}^{n\times n}$, $B_p \in \mathbb{R}^{n\times m}$, and $M_p \in \mathbb{R}^{n\times q}$. The matrix $K(t) = \text{diag}(k_1(t), \ldots, k_m(t))$ is comprised of scalar functions $k_i(t)$ which satisfy $0 \le k_i(t) < 1$. These model a decrease in effectiveness of a particular actuator: thus, if $k_i(t) = 0$, the ith actuator is working perfectly, whereas if $k_i(t) > 0$, some level of fault is present. Since, by assumption, $k_i(t) < 1$, this excludes the possibility of the actuators failing completely (although this issue will be addressed in detail separately later in the paper). Without loss of generality, it can be assumed that the input distribution matrix B_p has full rank, and the pair (A_p, B_p) is controllable. The function $\xi(t, x_p)$ is assumed to be unknown but bounded and represents uncertainty in the system. Here, it is assumed to satisfy

$$\|\xi(t, x_p)\| < \mathtt{C}_1 \|x_p(t)\| + \mathtt{C}_2 \tag{4}$$

where $\mathtt{C}_1$ and $\mathtt{C}_2$ are known constants. This uncertainty structure has been considered in [4, Sec. 3.6].

A. Sliding-Mode Controller Design

Integral action [4] will be included to add a tracking facility for the two controlled outputs FPA and V_{tas}. The uncertain faulty system from (3) has been augmented with integral action states $x_d \in \mathbb{R}^m$ satisfying

$$\dot{x}_d(t) = y_c(t) - C_c x_p(t) \tag{5}$$

where the differentiable signal $y_c(t)$ satisfies

$$\dot{y}_c(t) = \Gamma\left(y_c(t) - Y_d\right) \tag{6}$$

where $\Gamma \in \mathbb{R}^{m\times m}$ is a stable design matrix and Y_d is a constant demand vector. Augmenting the states from (3) with the integral action states and defining $x = \text{col}(x_d, x_p)$, it follows that

$$\dot{x}(t) = Ax(t) + Bu(t) + B_d y_c(t) - BK(t)u(t) + M\xi(t,x) \tag{7}$$

where

$$\begin{aligned} A &= \begin{bmatrix} 0 & -C_c \\ 0 & A_p \end{bmatrix} \\ B &= \begin{bmatrix} 0 \\ B_p \end{bmatrix} \\ B_d &= \begin{bmatrix} I_m \\ 0 \end{bmatrix} \\ M &= \begin{bmatrix} 0 \\ M_p \end{bmatrix}. \end{aligned} \tag{8}$$

Since the pair (A_p, B_p) is controllable, if (A_p, B_p, C_c) does not have any invariant zeros at the origin, then (A, B) is controllable [4]. For the later analysis, define an augmented version of b_s from (1) as

$$B_s = \begin{bmatrix} 0 \\ b_s \end{bmatrix}. \tag{9}$$

Although B_s does not directly appear in (7), it represents the distribution matrix associated with (7) when the horizontal stabilizer is employed as a "backup" control surface if a total failure in the elevator occurs. Define as a switching function

$$s(t) = Sx(t) \tag{10}$$

as a linear combination of the states, where $S \in \mathbb{R}^{m\times(n+m)}$ is full rank. If a control law can be developed that forces the closed-loop trajectories onto the surface $s(t) = 0$ in finite time (despite faults) and constrains the states to remain there, then an ideal sliding motion is said to have been attained [4]. Suppose the matrix S is designed so that the square matrix SB is nonsingular (in practice, this is easily accomplished, since B is full rank and S is a free parameter). Then, it is well known that the ideal sliding motion is given by

$$\dot{x}(t) = \left(I_{(n+m)} - B(SB)^{-1}S\right)\left(Ax(t) + M\xi(t,x) + B_d y_c(t)\right) \tag{11}$$

for all $t \geq t_s$ and $Sx(t_s) = 0$ [4]. It can be seen from (11) that the sliding motion is a control-independent free motion which depends on the choice of sliding surface. If $M_p \in \text{Im}(B_p)$, i.e., M_p belongs to the range space of the matrix B_p, then $(I_{(n+m)} - B(SB)^{-1}S)M = 0$, and the sliding motion is independent of the uncertainty. Several approaches have been proposed in the literature for the design of the matrix S including quadratic minimization, eigenvalue placement, eigenstructure assignment, and linear matrix inequality (LMI) methods (see, for example, [4, ch. 4]). Furthermore, without loss of generality, the surface can always be designed so that $SB = I_m$.

The proposed control law comprises two components: a linear component to stabilize the nominal linear system and a discontinuous component. Specifically

$$u(t) = u_l(t) + u_n(t) \tag{12}$$

where the linear component is given by

$$u_l(t) = \underbrace{-(SB)^{-1}(SA - \Phi S)}_{L} x(t) \underbrace{-(SB)^{-1}SB_d}_{L_d} y_c(t) \tag{13}$$

where $\Phi \in \mathbb{R}^{m\times m}$ is any stable design matrix and u_n is a discontinuous component which is a function of s.

In this paper, the choice of the nonlinear term $u_n(t)$ is facilitated by the choice of S for which $SB = I_m$, which effectively decouples the components of the sliding surface and associates with each a particular control input. Componentwise, the proposed control structure has the form

$$u_i(t) = u_{l_i}(t) - (\rho_i(t) + \eta_i)\,\text{sign}\,(s_i(t)), \quad i = 1, \ldots, m \tag{14}$$

where η_i are positive constants,[1] $u_{l_i}(t)$ is the ith component of $u_l(t)$, and $s_i(t)$ is the ith component of $s(t) = Sx(t)$. It is easy to see from (13) that $u_{l_i}(t)$ is bounded by $|u_{l_i}(t)| < l_1\|x(t)\| + l_2$, where l_1 and l_2 are known positive constants. The gains $\rho_i(\cdot)$ in each of the control channels are defined as

$$\rho_i(t) = r_i(t)\left(\bar{r}_{(i,1)}\|x(t)\| + \bar{r}_{(i,2)}\right) \tag{15}$$

where

$$\bar{r}_{(i,1)} := (l_1 + \|S_i M\|\mathtt{C}_1), \quad \bar{r}_{(i,2)} := (l_2 + \|S_i M\|\mathtt{C}_2) \tag{16}$$

and the constants $\mathtt{C}_1$ and $\mathtt{C}_2$ are from (4). The variables $r_i(t)$ are adaptive gains that vary according to

$$\dot{r}_i(t) = \alpha_i\left(\bar{r}_{(i,1)}\|x(t)\| + \bar{r}_{(i,2)}\right) D_\epsilon\left(|s_i(t)|\right) - \beta_i r_i(t) \tag{17}$$

where $r_i(0) = 0$ and the α_i and β_i are positive design constants. The function $D_\epsilon : \mathbb{R} \mapsto \mathbb{R}$ is the nonlinear function

$$D_\epsilon(s) = \begin{cases} 0, & \text{if } |s| < \epsilon \\ s, & \text{otherwise} \end{cases} \tag{18}$$

where ϵ is a positive scalar. (This function is also considered in [23]). Here, ϵ is set to be small and helps define a boundary layer about the surface $\mathcal{S} = \{x(t) : Sx(t) = 0\}$ inside which

[1]The η_i could be chosen as functions of the state, sufficiently large to bound the uncertainty in the fault-free case when $K(t) = 0$.

an acceptably close approximation to ideal sliding takes place. Provided the states evolve with time inside the boundary layer, no adaptation of the switching gains takes place. If a fault occurs that starts to make the sliding motion degrade so that the states evolve outside the boundary layer, i.e., $|s_i(t)| > \epsilon$, then the dynamic coefficients $r_i(t)$ increase in magnitude [according to (17)] to force the states back into the boundary layer around the sliding surface.

Remark: In a fault-free situation, it is not necessary and indeed is not advisable to have a large gain on the switched term—therefore, ideally, the term $\rho(\cdot)$ should only adapt to the onset of a fault and react accordingly. This adaptation scheme differs from the one in [22] and is more akin to the scheme given in [23]. The choice of the design parameters η_i, α_i, β_i, and ϵ depends on the closed-loop performance specifications and requires some design iteration. In general, the η_i need to be chosen as the nominal (no-fault) gains for the nonlinear component of the control law (14) to ensure that sliding occurs in the fault-free system. The parameter ϵ is chosen to be small to form a boundary layer about $\mathcal{S}$, but not too small to cause "false alarms" and unnecessary increases in $\rho_i(t)$. Thus, ϵ dictates how sensitive the adaptive gains $r_i(t)$ are to changes in $s(t)$. The gain α_i dictates the rate at which the adaptive gain $r_i(t)$ increases in reaction to faults: a large value for α_i indicates a fast increase of $r_i(t)$. On the other hand, β_i dictates the rate at which $r_i(t)$ decreases to the nominal gain η_i when the fault has been rectified. A relationship between ϵ, η_i, α_i, and β_i will be determined in the proof of the proposition that follows. The choice of these design parameters will be discussed further in Section III-B. The following proposition shows that the gain functions are bounded and motion inside a boundary layer around $\mathcal{S}$ is obtained.

Proposition 1: Consider the potentially faulty augmented system represented by (7) with the control law in (14); then, each of the components $r_i(t)$ remain bounded and the switching states $s(t)$ enter a boundary layer around $\mathcal{S}$ in finite time.

Proof: Consider $\bar{k} = \max\{k_1(t), \ldots, k_m(t)\}$. Notice that by assumption $\bar{k} < 1$. From the decoupled structure which results from $SB = I_m$, it follows that

$$\begin{aligned}\dot{s}_i = &-\phi_i s_i - (1-k_i(t))\,(\rho_i(t)+\eta_i)\,\mathrm{sign}(s_i)\\ &- k_i(t)u_{l_i}(t) + S_i M\xi(t,x)\end{aligned} \tag{19}$$

where it has been assumed that $\Phi = \mathrm{diag}(-\phi_1, \ldots, -\phi_m)$ and the ϕ_i are positive scalars. Therefore

$$\begin{aligned}s_i\dot{s}_i \le &-\phi_i s_i^2 - (1-\bar{k})\,(\rho_i(t)+\eta_i)\,|s_i|\\ &+ s_i\left(S_i M\xi(t,x) - k_i(t)u_{l_i}(t)\right).\end{aligned} \tag{20}$$

Using (16) and the fact that $\bar{k} = 1-(1-\bar{k})$, by construction

$$\begin{aligned}&|(S_i M\xi(t,x) - k_i(t)u_{l_i}(t))|\\ &\quad\le |S_i M\xi(t,x)| + \bar{k}\,|u_{l_i}(t)|\\ &\quad\le \left(\bar{r}_{(i,1)}\,\|x(t)\| + \bar{r}_{(i,2)}\right) - (1-\bar{k})\,|u_{l_i}(t)|\end{aligned} \tag{21}$$

for $i = 1, \ldots, m$ since, from (4), $\|\xi(t,x)\| < \mathtt{C}_1\|x(t)\| + \mathtt{C}_2$. Define a scalar

$$\zeta := 1/(1-\bar{k}) > 0 \tag{22}$$

and a component Lyapunov function

$$V_i = \frac{1}{2}\left\{s_i^2 + \frac{1}{\alpha_i}(1-\bar{k})\,(r_i(t)-\zeta)^2\right\} \tag{23}$$

where α_i is the positive scalar from (17). Clearly, $V_i(\cdot)$ is positive definite with respect to s_i, the adaptive gain errors $r_i(t)-\zeta$, and is radially unbounded. Taking derivatives

$$\dot{V}_i = s_i\dot{s}_i + \frac{1}{\alpha_i}(1-\bar{k})\,(r_i(t)-\zeta)\,\dot{r}_i(t) \tag{24}$$

then, substituting from (15), (17), (20), and (21) into the above and using the fact that $(1-\bar{k})\zeta = 1$, it follows that

$$\begin{aligned}\dot{V}_i \le &-\phi_i s_i^2 - |s_i|(1-\bar{k})\,(\eta_i + |u_{l_i}(t)|)\\ &- |s_i|(1-\bar{k})\left(\bar{r}_{(i,1)}\,\|x(t)\| + \bar{r}_{(i,2)}\right)\\ &\times (r_i(t)-\zeta) + \frac{1}{\alpha_i}(1-\bar{k})\,(r_i(t)-\zeta)\\ &\times \left(\alpha_i\left(\bar{r}_{(i,1)}\,\|x(t)\| + \bar{r}_{(i,2)}\right) D_\epsilon\left(|s_i(t)|\right) - \beta_i r_i(t)\right).\end{aligned} \tag{25}$$

If $|s_i| > \epsilon$, then $D_\epsilon(|s_i|) = |s_i|$ and so substituting into (25) and simplifying terms yields

$$\begin{aligned}\dot{V}_i \le &-\phi_i s_i^2 - |s_i|(1-\bar{k})\,(\eta_i + |u_{l_i}(t)|)\\ &- \frac{\beta_i}{\alpha_i}(1-\bar{k})\,(r_i(t)-\zeta)\,r_i(t).\end{aligned} \tag{26}$$

Notice by construction that $\bar{k} < 1$ and $r_i(t) \ge 0$. Further manipulation of (26) and using (22) yields

$$\begin{aligned}\dot{V}_i \le &-\phi_i s_i^2 - |s_i|(1-\bar{k})\,(\eta_i + |u_{l_i}(t)|)\\ &- \frac{\beta_i}{\alpha_i}(1-\bar{k})\left(\frac{1}{2}\zeta - r_i(t)\right)^2 + \frac{\beta_i}{4\alpha_i(1-\bar{k})}\end{aligned} \tag{27}$$

since expanding the quadratic term on the right-hand side of (27) gives (26). If $|s_i| > \epsilon$, then $|s_i|(1-\bar{k})\eta_i \ge (1-\bar{k})\epsilon\eta_i$. The quantities ϵ, η_i, α_i, and β_i are design parameters and, so, if they are chosen to satisfy

$$(1-\bar{k})\epsilon\eta_i \ge \frac{\beta_i}{4\alpha_i(1-\bar{k})} \tag{28}$$

then

$$\dot{V}_i \le -\phi_i s_i^2 - |s_i|(1-\bar{k})\,|u_{l_i}(t)| - \frac{\beta_i}{\alpha_i}(1-\bar{k})\left(\frac{1}{2}\zeta - r_i(t)\right)^2 \le 0. \tag{29}$$

If $|s_i| < \epsilon$, then $D_\epsilon(|s_i|) = 0$, and thus substituting into (25) and simplifying terms yields

$$\begin{aligned}\dot{V}_i \le &-\phi_i s_i^2 - |s_i|(1-\bar{k})\,(\eta_i + |u_{l_i}(t)|)\\ &- |s_i|(1-\bar{k})\left(\bar{r}_{(i,1)}\,\|x(t)\| + \bar{r}_{(2,i)}\right)(r_i(t)-\zeta)\\ &- \frac{\beta_i}{\alpha_i}(1-\bar{k})\,(r_i(t)-\zeta)\,r_i(t).\end{aligned} \tag{30}$$

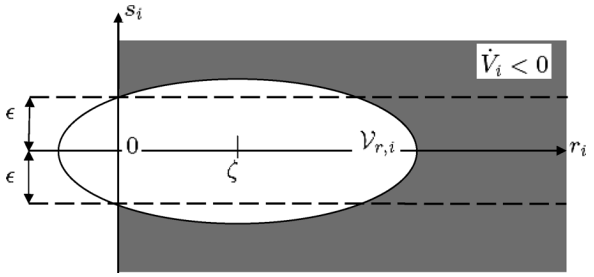

Fig. 1. Level set of the Lyapunov functions V_i.

Notice again by construction that $\bar{k} < 1$ and $r_i(t) \geq 0$, and, therefore, for $|s_i| < \epsilon$ and $r_i(t) > \zeta$, it follows that $\dot{V}_i < 0$. Define a rectangle in $\mathbb{R}^2$ as

$$\mathcal{R}_i = \{(s_i, r_i) \,||s_i| \leq \epsilon, 0 \leq r_i \leq \zeta\}\,. \tag{31}$$

Also define $\mathcal{R}_+ = \{(s_i, r_i) | r_i \geq 0\}$. By construction of the adaptive gains, $r_i(t) \geq 0$ for all time, and so the trajectory of $(s_i(t), r_i(t)) \in \mathcal{R}_+$ for all time, and so outside $\mathcal{R}_i \cap \mathcal{R}_+ = \mathcal{R}_i$, from (27) and (30), the derivative of the Lyapunov function $\dot{V}_i < 0$. Let $\mathcal{V}_{r,i}$ denote the truncated ellipsoid

$$\mathcal{V}_{r,i} = \{(s_i, r_i) | V_i(s_i, r_i) \leq r\} \cap \mathcal{R}_+$$

where $V_i(\cdot)$ is defined in (23). Because $\mathcal{R}_i$ from (31) is a compact set, $\exists$ a unique $r_{i,0} > 0$ s.t. $r_{i,0} = \min\{r \in \mathbb{R}_+ | \mathcal{R}_i \subset \mathcal{V}_{r,i}\}$ and, in fact, $r_{i,0} = (1/2)(\epsilon^2 + (\zeta/\alpha_i))$. As shown in Fig. 1, since $\mathcal{R}_i \subset \mathcal{V}_{r_{i,0}}$, it follows outside $\mathcal{V}_{r_{i,0}}$ the derivative of the Lyapunov function $\dot{V}_i < 0$, and thus $\mathcal{V}_{r_{i,0}}$ is an invariant set which is entered in finite time t_0. Since $\mathcal{V}_{r_{i,0}}$ is entered in finite time, $V_i(s_i, r_i) \leq r_{i,0}$ for all $t > t_0$, which implies $|s_i| \leq \sqrt{2r_{i,0}}$ for all time $t > t_0$, and hence s_i enters and remains in a boundary layer of size $\sqrt{2r_{i,0}}$ around the ideal sliding surface $\mathcal{S}$. ■

From the arguments above, for an appropriate choice of α_i, β_i, and ϵ, close approximation to ideal sliding can be maintained even in the presence of faults. The reduced-order sliding motion is then governed by (11). The motion depends on the uncertainty, but using arguments similar to those in [4, 3.6], for a sufficiently small $\mathtt{C}_1$, ultimate boundedness of the states $x(t)$ can be proved.

Remarks:

- If $\epsilon = 0$ and $\beta_i = 0$, then ideal sliding can be guaranteed since it follows from (26) that the Lyapunov derivative $\dot{V}_i(s) \leq -\phi_i s_i^2 - |s_i|(1 - \bar{k})(\eta_i + |u_{l_i}(t)|)$. This means that ideal sliding can be attained and maintained in finite time. However, this adaptive scheme has disadvantages in practice since the gains $r_i(t)$ may become unbounded in the presence of noise [22].
- The adaptive gains act as a measure of severity of the actuator fault. Once the adaptive gain $\rho_i(t)$ from (15) exceeds a predetermined maximum value $\rho_{\max,i}$, a very severe fault or failure can be detected, and a "backup" control strategy can be initiated if required.
- From (22), as $\bar{k} \to 1$, ζ becomes infinitely large. In the case of total failure ($k_i(t) = 1 \Rightarrow \bar{k} = 1$), an alternative control strategy must be employed.

1) Sliding-Mode Hyperplane Design: The first step in sliding-mode controller design is the selection of the sliding surface matrix S. One methodology is the quadratic cost function approach [4], [20]. In this paper, a novel modification of this approach is considered to take into account the occurrence of failures. The design approach adopted here is described specifically for the aircraft system. However, its underlying philosophy is generic and could be adopted in other systems. First consider the problem of designing a sliding surface matrix S for the nominal linear system associated with (7). Assume that there are no faults (i.e., $K(t) = 0$) and there is no reference demand ($y_c(t) = 0$).[2] Also, for the purpose of design, ignore the uncertainty term. For this nominal linear system, as in [20], consider the problem of minimizing the quadratic performance index

$$J = \frac{1}{2}\int_{t_s}^{\infty} x(t)^{\mathrm{T}} Q x(t) dt \tag{32}$$

where Q is a symmetric positive definite (s.p.d) matrix and t_s is the time at which the sliding motion commences. Define a change of coordinates given by

$$z(t) = T_r x(t) \tag{33}$$

where T_r is an orthogonal matrix, so that the system in (7) is in regular form [20], i.e.,

$$T_r A {T_r}^T = \begin{bmatrix} A_{11} & A_{12} \\ A_{21} & A_{22} \end{bmatrix}, \quad T_r B = \begin{bmatrix} 0 \\ B_2 \end{bmatrix}$$

where $A_{11} \in \mathbb{R}^{n \times n}$, $B_2 \in \mathbb{R}^{m \times m}$. Also, assume that, (in regular form) the matrix $T_r Q T_r^{\mathrm{T}}$ associated with (32) has a block-diagonal structure so that $T_r Q T_r^{\mathrm{T}} = \mathrm{diag}(Q_1^{\mathrm{T}} Q_1, Q_2^{\mathrm{T}} Q_2)$, where $Q_2^{\mathrm{T}} Q_1 = 0$ and the matrix $Q_2^{\mathrm{T}} Q_2 \in \mathbb{R}^{m \times m}$ is nonsingular. It follows that

$$J = \frac{1}{2}\int_{t_s}^{\infty} z_1(t)^{\mathrm{T}} Q_1^{\mathrm{T}} Q_1 z_1(t) + z_2(t)^{\mathrm{T}} Q_2^{\mathrm{T}} Q_2 z_2(t) dt \tag{34}$$

where $z = \mathrm{col}(z_1, z_2)$ with $z_1 \in \mathbb{R}^n$. Because of the assumption of regular form, under nominal fault-free operation, the differential equation constraint (7), while sliding, may be written as

$$\dot{z}_1(t) = A_{11} z_1(t) + A_{12} z_2(t) \tag{35}$$

where the "virtual control" z_2 satisfies

$$\mathcal{K} z_1 + z_2 = 0. \tag{36}$$

Here, (36) represents the hyperplane equation $Sx = 0$ for $S T_r^{\mathrm{T}} = S_2[\mathcal{K}\ I_m]$, where $S_2 \in \mathbb{R}^{m \times m}$ and is nonsingular. Substituting for z_2 from (36) into (35) gives an autonomous reduced-order sliding motion. The matrix $\mathcal{K}$ must be chosen to make $(A_{11} - A_{12}\mathcal{K})$ stable. This is always possible since (A_{11}, A_{12}) is controllable if (A, B) is controllable. As argued in [2], the optimal cost is given by $J = z_1(t_s)^{\mathrm{T}} P_c z_1(t_s)$, where

[2]Although as argued in [4, 7.3.3], since $y_c(t) \to Y_d$, the effect of the demand signal can be removed by a change of coordinates that considers the system states relative to their steady-state values.

P_c is the symmetric positive definite solution to the Riccati equation

$$P_c A_{11} + A_{11}^{\mathrm{T}} P_c - P_c A_{12} \left(Q_2^{\mathrm{T}} Q_2\right)^{-1} A_{12}^{\mathrm{T}} P_c + Q_1^{\mathrm{T}} Q_1 = 0 \quad (37)$$

where $z_1(t_s)$ is the value of the state component z_1 at the time at which sliding occurs and the optimal choice of $\mathcal{K} = (Q_2^{\mathrm{T}} Q_2)^{-1} A_{12}^{\mathrm{T}} P_c$. This problem can be posed as an LMI optimization: minimize trace (X^{-1}) subject to

$$\begin{bmatrix} A_{11}X + XA_{11}^{\mathrm{T}} - A_{12}N - N^{\mathrm{T}}A_{12}^{\mathrm{T}} & (Q_1X - Q_2N)^{\mathrm{T}} \\ Q_1X - Q_2N & -I \end{bmatrix} < 0, \quad X > 0 \quad (38)$$

where $N := \mathcal{K}X$. As argued in [2, p. 114], any solution to (38) satisfies $X^{-1} \geq P_c$. Consequently, $\mathrm{trace}(X^{-1}) \geq \mathrm{trace}(P_c)$, and hence the minimization process results in $X^{-1} = P_c$.

In the "backup" case, the input distribution matrix is perturbed by the change in actuator. Now the new input distribution matrix $\tilde{B}$ (say) is formed from replacing the first column from B in (8) associated with the elevator, with B_s in (9) which is associated with the horizontal stabilizer. In the regular form coordinates

$$T_r \tilde{B} = \begin{bmatrix} B_1 \\ B_2 R \end{bmatrix}$$

where $B_1 \in \mathbb{R}^{n \times m}$ and $R \in \mathbb{R}^{m \times m}$. Provided a sliding motion can be maintained with the new actuator set, in the regular form coordinates, the uncertain reduced order motion can be represented as

$$\dot{z}_1(t) = (A_{11} - A_{12}\mathcal{K}) z_1(t) + M_1 \xi + B_1 u_{\mathrm{eq}}(t) \quad (39)$$

instead of (35) and (36), where $u_{\mathrm{eq}}(t)$ is the equivalent control signal necessary to maintain a sliding motion on $\mathcal{S}$ [20] and M_1 represents the top n rows of $T_r M$ i.e., the unmatched uncertainty distribution matrix in the regular form coordinates. The signal $u_{\mathrm{eq}}(t)$ will be a function of the states z_1 and will include the effects of any additional mismatched disturbances resulting from the failure (such as turning moments generated from stuck actuators). The objective is to minimize the effect of $u_{\mathrm{eq}}(t)$ on the nominal performance of the system in (39) in an $\mathcal{L}_2$ sense [10]. Under the constraint that a common Lyapunov function for both the quadratic cost problem and the $\mathcal{L}_2$ gain problem is sought, from the Bounded Real Lemma [2], the $\mathcal{L}_2$ gain between $u_{\mathrm{eq}}(t)$ and z_1 is less than γ if

$$\begin{bmatrix} A_{11}X + XA_{11}^{\mathrm{T}} - A_{12}N - N^{\mathrm{T}}A_{12}^{\mathrm{T}} & [B_1\ M_1] & X \\ [B_1\ M_1]^{\mathrm{T}} & -\gamma I & 0 \\ X & 0 & -\gamma I \end{bmatrix} < 0. \quad (40)$$

The overall optimization problem used here is: minimize $(a_1 \mathrm{trace}(Z) + a_2 \gamma)$ subject to

$$\begin{bmatrix} -Z & I_n \\ I_n & -X \end{bmatrix} < 0 \quad (41)$$

in addition to (38) and (40). The matrix variable Z is a "slack variable" that satisfies $Z > X^{-1}$ and so $\mathrm{trace}(Z)$ bounds $\mathrm{trace}(X^{-1})$. Here, a_1 and a_2 are positive scalars that determine the relative weighting between the quadratic cost and $\mathcal{L}_2$ problem. This represents a convex optimization problem in terms of X, Z, N, and γ and can be solved using standard LMI packages. The matrix that determines the hyperplane is computed as $\mathcal{K} = NX^{-1}$ and, finally (in the original coordinates), the matrix

$$S = S_2 [\mathcal{K} \quad I_m] T_r. \quad (42)$$

The nonsingular matrix S_2 is then chosen to ensure $SB = I_m$. Although the development above is specific to the B747 backup stabilizer scenario, the approach is more flexible and could be used in more general situations.

B. Actuator Fault-Tolerant Controller for the B747-100/200

This subsection describes the actuator fault-tolerant controller designed for the B747-100/200 aircraft. The controller is designed for longitudinal axis control in the "up and away" flight envelope [6]. The main objective is to obtain tracking of flight path angle (FPA) and true air speed V_{tas}. The settling time when there is no fault/failure should be approximately 20 s for FPA and 45 s for V_{tas}. If a fault/failure occurs, the tracking requirement is 30 s for FPA with no difference in the V_{tas} tracking. These specifications are adopted from [6].

The weighting matrix

$$T_r Q T_r^{\mathrm{T}} = \mathrm{diag}\left(0.5 I_2, \quad \begin{bmatrix} 2 & -1 \\ -1 & 1 \end{bmatrix}, \quad 5, \quad 20\right). \quad (43)$$

The last two elements of $T_r Q T_r^{\mathrm{T}}$ multiply the z_2 term in (34) and thus weight the "virtual control" term. Thus, by analogy to a more typical LQR framework, they affect the speed of response of the closed-loop system. The last state is weighted heavily to reduce the gains in the engine channels. The first two terms in (43) are associated with the integral action states and are less heavily weighted. The nondiagonal term in (43) arises from the fact that the FPA is the quantity of interest. In the following design, the parameters $a_1 = a_2 = 1$. Here, an equal weight on the quadratic cost performance and the $\mathcal{L}_2$ robustness has been chosen to represent equal importance of the nominal (no-fault) performance and robustness when a total actuator failure occurs. In this example, the choice of a_2 is not crucial because the degree of mismatch between B and $\tilde{B}$, represented by $\|B_1\|$, is small. The LMI optimization software gives a unique solution for $\mathcal{K}$ in (42). The original sliding surface matrix S obtained from the optimization software (42) has been scaled using S_2 in order that $SB = I_2$. The poles associated with the reduced-order sliding motion are $\{-0.6786, -0.3566 \pm 0.3802i, -0.1584\}$. From (13), the stable matrix has been chosen as $\Phi = -I_2$ which gives faster poles than those associated with the reduced-order sliding motion. The prefilter matrix from (6) has been designed to be $\Gamma = \mathrm{diag}(-0.2400, -0.1250)$. This may be viewed as representing the ideal response in the FPA and the V_{tas} channels. Again, the FPA response is faster than the V_{tas} response. In the simulations, the discontinuity in the nonlinear control term has been smoothed by using a sigmoidal approximation $s/(|s| + \delta)$, where the fixed scalar $\delta = 0.01$ (see, for example, [4, § 3.7]). This removes the discontinuity and introduces a further degree of tuning to accommodate the actuator rate limits, especially

during actuator fault or failure conditions. The initial fixed gains for the "backup" controller (using the horizontal stabilizer) are given by $\rho_{s,1} = 0.4$ and $\rho_{s,2} = 0.05$. Here, the smoothing parameter is chosen as $\delta_s = 0.1$. The larger value of δ_s is used to accommodate the smaller positional movement and lower rate limits of the horizontal stabilizer. In this paper, only the gains in the elevator channel are allowed to adapt: the gains associated with the thrust channel are fixed. When employing the adaptive gain for the controller from (14), it was found for this particular example that the $\bar{r}_{(i,1)}(t)$'s in (16) have no significant effect on the closed-loop performance, and so $l_1 = \mathtt{C}_1 = 0$ was chosen and therefore $\bar{r}_{(i,1)}(t) \equiv 0$. The parameters l_2 and $\mathtt{C}_2$ have been chosen as $l_2 = 0.5$ and $\mathtt{C}_2 = 0.9117$ and therefore $\bar{r}_{(i,2)}(t) \equiv 1$. The upper and lower limits for $\rho_1(t)$ have been chosen as $\rho_{\max,1} = 5$ and $\rho_{\min,1} = \eta_1 = 0.2$, respectively. Here, $\eta_1 = 0.2$ is chosen to be larger than the uncertainty in the no-fault condition. The choice of $\rho_{\max,1}$ dictates how fast a severe or total failure can be detected. Here, $\rho_{\max,1}$ has been chosen to be sufficiently large to compensate for the worst case fault on the elevator (before the switch to stabilizer is activated) at a 70% decrease in effectiveness. The adaptation parameters are $\alpha_1 = 600$ and $\beta_1 = 0.02$ and the tolerance $\epsilon = 0.0005$. Appropriate values for α_1, β_1, and ϵ involve some design iteration. The parameter ϵ was chosen to be able to tolerate the variation in $s(t)$ due to normal changes in flight conditions but small enough to enable the adaptive gain to be sensitive to deviations from zero in the switch term s_1 when a fault or severe disturbance occurs. The term α_1 dictates the rate at which $\rho(t)$ increases and reacts to the faults. Here, it needs to be large to enable small changes in s_1 to cause significant changes in the gain so that the control system reacts quickly to the onset of a fault. From (28), $(1-\bar{k})\epsilon\eta_i = 3.0 \times 10^{-5}$ and $\beta_i/(4\alpha_i(1-\bar{k})) = 2.78 \times 10^{-5}$ and therefore the condition in Proposition 1 is satisfied.

1) Actuator FTC Simulation Results: The simulations presented in this paper are all based on the *full 77 state nonlinear model*. For the "up and away" flight condition, the elevator is used to track FPA demands. As in the work of Ganguli *et al.* [6], this paper only considers faults/failures to the elevator. The simulations have been conducted at an altitude of 4000 m and a V_{tas} of 184 m/s. The reference command requests a change in flight path angle of 3° for 20 s followed by a 20-m/s change in speed over a period of 45 s (in two steps). The command sequence for the FPA demand is then reversed after 250 s so that the aircraft is returned to (approximately) the initial flight conditions. The "effectiveness gain" $k_1(t)$ has been implemented as a simple but unknown (as far as the controller is concerned) gain between the output of the controller block and the actuator dynamics. These simple tests indicate the effect of a loss of efficiency of the elevator due to damage or faults. Fig. 2 shows the results of nonlinear simulations for various fault conditions: a nominal (no-fault) period for the first 150 s, followed by degradation of the elevator effectiveness (150–260 s), and, finally, total failure (260–400 s). From 150–260 s, as shown in Fig. 2(e) and (j), the elevator effectiveness degrades from (normal) 100% to 40% effectiveness. Subsequently, the elevator develops floating and/or lock type actuator failures at 260 s. These simulate total failure of the elevator and therefore require stabilization of the aircraft using the backup controller (which uses the horizontal stabilizer). The failure is set to occur during the descent (pitch down) manoeuvre at 260 s for both failure scenarios. To simulate a floating actuator type of failure, the elevator signal is replaced with the angle of attack signal [6]. This simulates the ineffectiveness of the elevator to provide a moment, and therefore the aircraft is unable to perform a pitch manoeuvre. Fig. 2(a) shows that FPA tracking performance is slightly degraded and the response is slower. Fig. 2(d) shows that the failure is detected at 261.71 s when the adaptive gain reaches its maximum set value. Some peaks can be seen in the horizontal stabilizer signal [see Fig. 2(c)] after activation due to the sudden change of control signal, but this stabilizes after a few seconds. *Once the controller is switched to the horizontal stabilizer, that surface is used for the remainder of the simulation.* Overall performance is satisfactorily maintained after detection of the failure and the change to the backup controller. To simulate lock failures, the elevator position is held at its value at 260 s. Fig. 2(f) shows that the FPA tracking is slightly degraded. Failure is detected at 262.62 s [see Fig. 2(i)], and the stabilizer is activated [see Fig. 2(h)]. Overall tracking performance is maintained.

IV. Sensor FTC

In the previous section, a controller was developed which copes with *actuator faults and failures*. The scheme assumes that accurate fault-free measurements of the states are available. Here, the possibility of *faulty measurements* in x_p will be considered. The idea is to use sliding-mode observers to reconstruct the fault signals and to use these signals to correct the measured values before they are used in the control law.

A. Preliminaries

This subsection introduces the preliminaries necessary for robust sensor fault reconstruction using sliding-mode observers. Consider an uncertain dynamical system affected by sensor faults described by

$$\dot{x}_p(t) = A_p x_p(t) + B_p u(t) + M_p \xi(t, x_p) \tag{44}$$

$$y(t) = x_p(t) + N_p f_o(t) \tag{45}$$

where $A_p \in \mathbb{R}^{n\times n}$, $B_p \in \mathbb{R}^{n\times m}$, $N_p \in \mathbb{R}^{n\times r}$, and $M_p \in \mathbb{R}^{n\times q}$ with $n > r$. Assume that the matrix N_p is full column rank and the function $f_o : \mathbb{R}_+ \to \mathbb{R}^r$ is unknown but bounded so that

$$\|f_o(t)\| \le \hat{a}(t) \tag{46}$$

where $\hat{a} : \mathbb{R}_+ \to \mathbb{R}_+$ is a known function. The signal $f_o(t)$ represents (additive) sensor faults and N_p represents a distribution matrix (with columns usually formed from the standard basis for $\mathbb{R}^n$), which indicates which of the sensors providing measurements are prone to possible faults. Notice that, in this special case, all of the states are assumed to be measured by sensors—which is normal for modern civil aircraft.

Remark: The assumption that only certain sensors are fault prone is a limitation. However, in practical situations, some sensors may be more vulnerable to damage or may be more sensitive or delicate in construction than others, and so such a situation is not unrealistic. Also certain key sensors may have

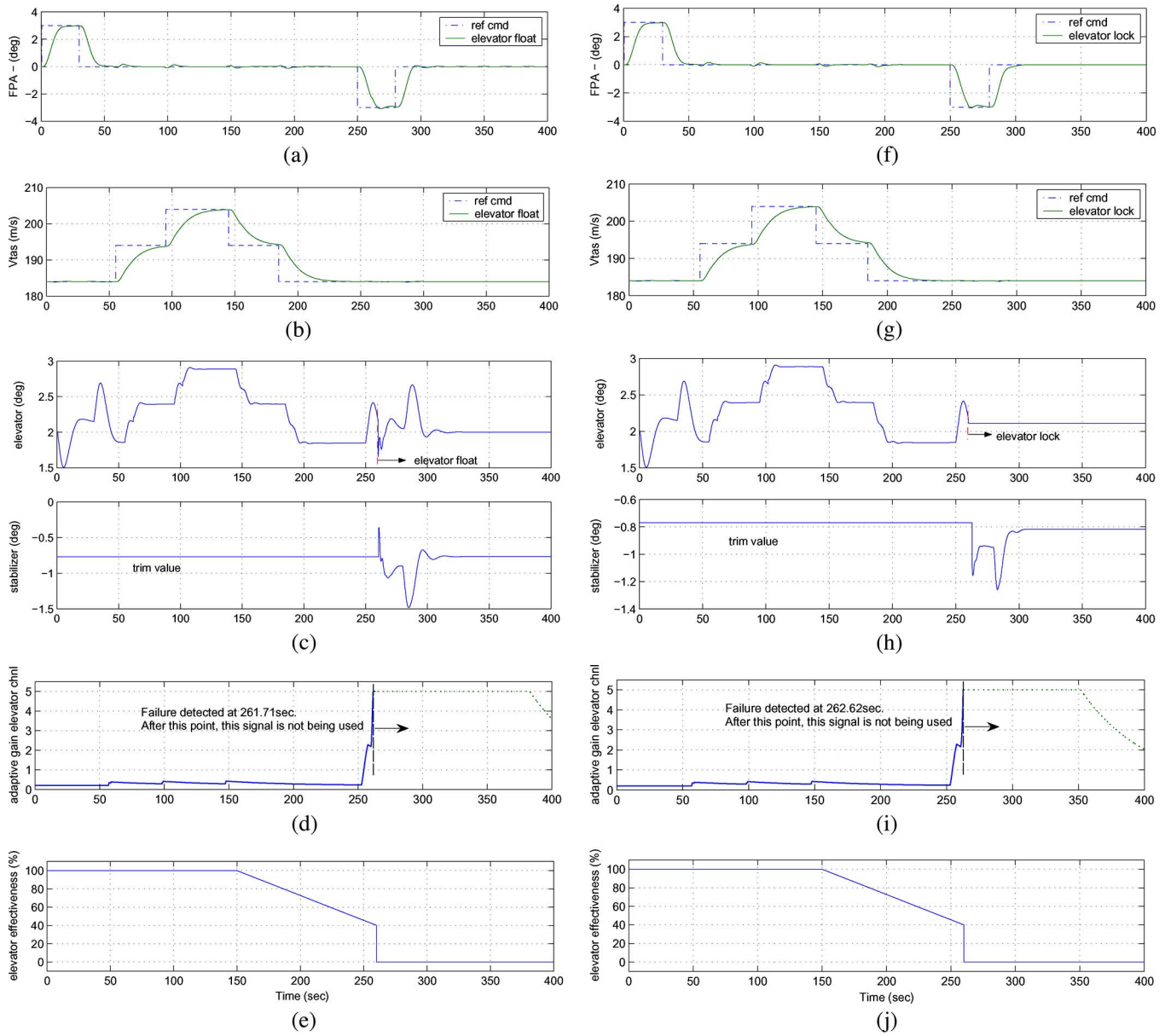

Fig. 2. Responses of nominal, fault, and failures (float and lock failures). (a) Float failure: FPA response. (b) Float failure: $V_{\rm tas}$ response. (c) Float failure: actuator positions (with trim value). (d) Float failure: the adaptive gain ρ_1. (e) Float failure: elevator effectiveness. (f) Lock failure: FPA response. (g) Lock failure: $V_{\rm tas}$response. (h) Lock failure: actuator positions (with trim value). (i) Lock failure: the adaptive gain ρ_1. (j) Lock failure: elevator effectiveness.

backups (hardware redundancy), and so essentially a fault-free signal can be assumed from a certain subset of the sensors.

The objective is to design a *sliding-mode* observer [4], [20] in order to *reconstruct* the faults $f_o(t)$. As argued in [19], an effective way to do this is to first introduce a filter. Consider a new state $x_f \in \mathbb{R}^n$ that is a filtered version of y, satisfying

$$\dot{x}_f(t) = -A_f x_f(t) + A_f\left(x_p(t) + N_p f_o(t)\right) \tag{47}$$

where $-A_f \in \mathbb{R}^{n\times n}$ is a stable matrix. Equations (44) and (47) can be combined to give a system of order $2n$ with states $x_a = \mathrm{col}(x_p, x_f)$ in the form

$$\dot{x}_a(t) = A_a x_a(t) + B_a u(t) + F_a f_o(t) + M_a \xi(t, x_p) \tag{48}$$
$$x_f(t) = C_a x_a(t) \tag{49}$$

for appropriate $A_a \in \mathbb{R}^{(2n)\times(2n)}$, $B_a \in \mathbb{R}^{(2n)\times m}$, $C_a \in \mathbb{R}^{n\times(2n)}$, $F_a \in \mathbb{R}^{(2n)\times r}$, and $M_a \in \mathbb{R}^{(2n)\times q}$. For the uncertain system in (48) and (49), a sliding-mode observer of the form

$$\dot{\hat{x}}_a(t) = A_a \hat{x}_a(t) + B_a u(t) - G_l e_y(t) + G_n \nu \tag{50}$$

will be considered. In (50), the discontinuous output error injection term

$$\nu = -\rho_o(t, y, u)\frac{P_o e_y}{\|P_o e_y\|} \quad \text{if } e_y \neq 0 \tag{51}$$

where $e_y(t) := C_a \hat{x}_a(t) - x_f(t)$ is the output estimation error and P_o is a s.p.d. matrix. The matrix G_l is a traditional Luenberger observer gain used to make $(A_a - G_l C_a)$ stable and G_n must be chosen to ensure the nonzero eigenvalues of $(I - G_n(C_a G_n)^{-1}_{C_a})A_a$ (i.e., the poles of the associated

reduced-order sliding motion) are stable. The scalar function $\rho_o(\cdot)$ must be an upper bound on the uncertainty and the faults; for details, see [19]. Edwards *et al.* [5] have shown that a sliding-mode observer of the form (50) and (51), which is completely insensitive to the fault $f_o(t)$, exists if and only if:

A1) $\operatorname{rank}(C_a F_a) = r$;

A2) no invariant zeros of (A_a, F_a, C_a) are in $\mathbb{C}_+$.

It can be shown that, provided the plant is open-loop stable, these conditions can always be met.[3] For an appropriate choice of $\rho_o(t, y, u)$ in (51), which must bound the uncertainty and the supremum of $\hat{a}(t)$ from (46), it can be shown that an ideal sliding motion takes place on $\mathcal{S}_o = \{e : C_a e = 0\}$ in finite time, where e is the state estimation error $(\hat{x}_a - x_a)$. For details see [19]. During the ideal sliding motion [4], [20], $e_y = \dot{e}_y = 0$, and the discontinuous signal ν must take on average a value to compensate for ξ and f_o to maintain sliding. The average quantity, denoted by ν_{eq}, is referred to as the *equivalent output error injection term* (the natural analog of the concept of equivalent control [20]). The signal ν_{eq} can be approximated to any degree of accuracy and is computable online as

$$\nu_\delta = -\rho_o(t, y, u)\frac{P_o e_y}{||P_o e_y|| + \delta_o} \tag{52}$$

where δ_o is a small positive scalar [4]. Consider as a fault reconstruction signal

$$\hat{f}_o := W\nu_\delta \tag{53}$$

where $W \in \mathbb{R}^{r\times n}$. In fact, only $r \times (n - r)$ elements in W are freely assignable since W must be chosen to ensure that $WC_aF_a = I_r$. For details, see [19]. Then, by straightforward manipulation, it can be shown that the fault reconstruction signal from (53) satisfies

$$\hat{f}_o(t) = f_o(t) + \hat{G}(s)\xi(t, x_p) \tag{54}$$

where $\hat{G}(s)$ is a transfer function matrix that depends on the plant matrices A_a and M_a, the observer matrix G_n, and the weighting matrix W. Tan and Edwards [19] propose minimizing the effect of ξ on the reconstruction $\hat{f}_o$ by minimizing the $\mathcal{L}_2$ gain between ξ and $\hat{f}_o$. Because the relationship between the two signals is the transfer function matrix $\hat{G}(s)$, this is equivalent to minimizing the $\mathcal{H}_\infty$ norm of $\hat{G}(s)$ [25]. With an appropriate change of variables, the problem of minimizing $\hat{\gamma} := ||\hat{G}(s)||_\infty$, whilst satisfying the requirements of a feasible sliding-mode observer design, can be cast as a well-defined convex optimization problem and efficiently solved using LMI methods [2]. In this paper

$$G_l := \hat{\gamma}_0 P^{-1} C_a^T \left(D_1 D_1^T\right)^{-1} \tag{55}$$

where $\hat{\gamma}_0$ is a positive design scalar (an upper bound on $\hat{\gamma}$) and $D_1 \in \mathbb{R}^{n\times n}$ is a design parameter (which may be viewed as a covariance-like matrix associated with sensor noise). The s.p.d. matrix $P \in \mathbb{R}^{(2n)\times(2n)}$ is a Lyapunov matrix for the state estimation error system from which P_o in (51) and (52) is derived. Details of the formulas and the change of coordinates used to obtain a convex optimization problem are given in [19].

[3]Open-loop stability is only a sufficient condition; more complicated necessary and sufficient conditions are discussed in [18], where unstable open-loop systems are considered.

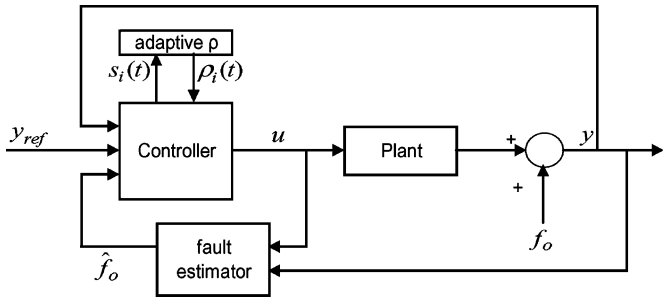

Fig. 3. Schematic of the sensor fault implementation.

A general configuration representing the proposed sensor FTC scheme that will be used in this paper is shown in Fig. 3. In this particular figure, the specific output of the FDI component is the sensor fault estimate $\hat{f}_o$. In active FTC, the information from the FDI scheme would trigger an online reconfiguration or adaptation of the control law. In this paper, the estimated sensor fault $\hat{f}_o$ will be used to correct the measured output signal so that $y - N_p\hat{f}_o$ will be the output of a "virtual sensor" that will be used in the control law calculations to generate u. Suppose the corrected output measurement is given by $\hat{x}_p$, and then

$$\hat{x}_p := y - N_p\hat{f}_o = x_p + N_p(f_o - \hat{f}_o). \tag{56}$$

Also, the integral action states from (5) are corrected so that

$$\dot{x}_d = y_c - C_c\hat{x}_p = y_c - C_c x_p - C_c N_p(f_o - \hat{f}_o). \tag{57}$$

After the coordinate change $x \mapsto T_r x = z$, and assuming for stability analysis purposes that $y_c \equiv 0$, then

$$\begin{bmatrix}\dot{z}_1\\ \dot{z}_2\end{bmatrix} = \begin{bmatrix}A_{11} & A_{12}\\ A_{21} & A_{22}\end{bmatrix}\begin{bmatrix}z_1\\ z_2\end{bmatrix} + \underbrace{\begin{bmatrix}M_1\\ M_2\end{bmatrix}}_{T_r M}\xi - \underbrace{\begin{bmatrix}B_d^1\\ B_d^2\end{bmatrix}}_{T_r B_d C_c N_p}(f_o - \hat{f}_o). \tag{58}$$

By construction

$$f_o - \hat{f}_o = -\hat{G}(s)\xi(t, x_p)$$

and suppose $\hat{G}(s)$ has a state-space realization $(\hat{A}, \hat{B}, \hat{C}, \hat{D})$ with states $\hat{e} \in \mathbb{R}^{(n-p)}$ which implies $f_o - \hat{f}_o = -\hat{C}\hat{e} - \hat{D}\xi$. During a sliding motion, since $\hat{x}$ is used in place of x in the control law, it follows that $\hat{s}(t) = S\hat{x} = 0$ and so

$$\begin{aligned} S\hat{x} = 0 &\Leftrightarrow ST_r^{\mathrm{T}}T_r x + S\hat{N}_p(f_o - \hat{f}_o) = 0\\ &\Leftrightarrow S_2[\mathcal{K} \quad I_m]z + S\hat{N}_p(f_o - \hat{f}_o) = 0 \end{aligned} \tag{59}$$

where $\hat{N}_p^{\mathrm{T}} = [0_{m\times m}\ N_p^{\mathrm{T}}]$ to account for the augmentation of the integral action states. From (59), during a sliding motion, we have

$$z_2(t) = -\mathcal{K}z_1(t) + S_2^{-1}S\hat{N}_p\left(\hat{C}\hat{e}(t) + \hat{D}\xi(t, x_p)\right). \tag{60}$$

Consequently, from (58), the reduced-order sliding motion is governed by

$$\begin{aligned} \dot{z}_1(t) =& (A_{11} - A_{12}\mathcal{K})z_1(t) + M_1\xi(t, x_p)\\ &+ \left(A_{12}S_2^{-1}S\hat{N}_p + B_d^1\right)\left(\hat{C}\hat{e}(t) + \hat{D}\xi(t, x_p)\right) \end{aligned} \tag{61}$$

$$\dot{\hat{e}}(t) = \hat{A}\hat{e}(t) + \hat{B}\xi(t, x_p). \tag{62}$$

By assumption, $\|\xi(t,x_p)\| \leq \mathtt{C}_1\|z_p(t)\| + \mathtt{C}_2$. Consequently, since $(\mathtt{C}_1\|z_p(t)\| + \mathtt{C}_2)^2 \leq 2\mathtt{C}_1^2\|z_p(t)\|^2 + 2\mathtt{C}_2^2$, it follows from (60) that

$$\begin{aligned}\|\xi(t,x_p)\|^2 &\leq 2\mathtt{C}_1^2\left(\|z_1(t)\|^2 + \|z_2(t)\|^2\right) + 2\mathtt{C}_2^2 \\ &\leq 2\mathtt{C}_1^2\left(\left(1+\|\mathcal{K}\|^2\right)\|z_1(t)\|^2 + \left\|S_2^{-1}S\hat{N}_p\hat{C}\right\|^2\|\hat{e}(t)\|^2 \right. \\ &\qquad \left. + \left\|S_2^{-1}S\hat{N}_p\right\|^2\|\hat{D}\|^2\|\xi(t,x_p)\|^2\right) + 2\mathtt{C}_2^2.\end{aligned}$$

Let $\alpha^2 := \max\{1+\|\mathcal{K}\|^2, \|S_2^{-1}S\hat{N}_p\hat{C}\|^2\}$. Using the fact that $\|\hat{G}(s)\|_\infty < \hat{\gamma} \Rightarrow \|\hat{D}\| < \hat{\gamma}$ means

$$\begin{aligned}\|\xi(t,x_p)\|^2 \leq 2\mathtt{C}_1^2\left(\alpha^2\left(\|z_1(t)\|^2 + \|\hat{e}(t)\|^2\right)\right. \\ \left. + \left\|S_2^{-1}S\hat{N}_p\right\|^2\hat{\gamma}^2\|\xi(t,x_p)\|^2\right) + 2\mathtt{C}_2^2. \quad (63)\end{aligned}$$

Suppose $2\mathtt{C}_1^2\hat{\gamma}^2\|S_2^{-1}S\hat{N}_p\|^2 < 1$, which will always be satisfied for a sufficiently small $\hat{\gamma}$. Then, rearranging (63) yields

$$\begin{aligned}\|\xi(t,x_p)\|^2 &\leq \left(\underbrace{\frac{2\mathtt{C}_1^2\alpha^2}{\left(1-2\mathtt{C}_1^2\hat{\gamma}^2\left\|S_2^{-1}S\hat{N}_p\right\|^2\right)}}_{\hat{\mathtt{C}}_1^2}\left\|\begin{bmatrix}z_1(t)\\ \hat{e}(t)\end{bmatrix}\right\|^2\right. \\ &\qquad \left. + \underbrace{\frac{2\mathtt{C}_2^2}{\left(1-2\mathtt{C}_1^2\hat{\gamma}^2\left\|S_2^{-1}S\hat{N}_p\right\|^2\right)}}_{\hat{\mathtt{C}}_2^2}\right) \\ &\leq \left(\hat{\mathtt{C}}_1\left\|\begin{bmatrix}z_1(t)\\ \hat{e}(t)\end{bmatrix}\right\| + \hat{\mathtt{C}}_2\right)^2. \quad (64)\end{aligned}$$

Notice that $\hat{\mathtt{C}}_1 \to 0$ as $\mathtt{C}_1 \to 0$, and so, as the plant uncertainty decreases, the uncertainty in (61) and (62) diminishes. If $\xi(t,x_p) \equiv 0$, then (61) and (62) are stable since both $A_{11} - A_{12}\mathcal{K}$ and $\hat{A}$ are stable by design. Consequently, using Lyapunov arguments similar to those in [4, § 3.6], there exists a value of $\mathtt{C}_1 > 0$ for which the system (61) and (62) retains stability.

B. Robust Sensor Fault Reconstruction of B747-100/200

Here, we describe the development of the fault reconstruction scheme for the *full nonlinear model* of the B747-100/200 aircraft. A key aspect of the design is to establish the matrix M_p from (44) which captures the discrepancy between the nonlinear and linear models. A much more accurate model is required here for analytical redundancy purposes than for the controller design. Prior to obtaining the matrix M_p, the second state (V_{tas}) has been scaled by 0.1, and therefore the plant system triple (A_p, B_p, C_p) is transformed by the transformation matrix given by $T_s = \text{diag}(1, 0.1, 1, 1)$. This has been done so that the magnitude of each of the states is comparable. Uniformly sampled data at 10 Hz was collected from the nonlinear (open-loop) simulation which was excited using a PRBS signal with amplitude 1° in the elevator channel. An estimate of the derivatives of each of the state space vector components was obtained numerically (offline), and an error vector $e_p := \dot{x} - Ax - Bu$ was then computed for each sample. In terms of the uncertainty model from (44), $\{e_p\} = M_p\{\xi\}$. Principal component analysis on the signals e_p using the singular value decomposition of the matrix $e_p^T e_p$ has been employed to compute M_p. This is based on the procedure proposed by Chen and Patton [3]. The singular values of the matrix $e_p^T e_p \in \mathbb{R}^{4\times 4}$ are given by {3.2332, 1.9011, 0.3644, 0.0001}. The first two are significantly larger than the last two, and so M_p has been chosen as the eigenvectors associated with the first two singular values, giving

$$M_p = \begin{bmatrix}-0.8562 & 0.4262\\ -0.3149 & -0.8786\\ -0.4049 & -0.2155\\ 0.0000 & -0.0000\end{bmatrix}. \quad (65)$$

Details of the justification of this appear in [3]. Note that the elements in the last row of M_p are small compared with the others. This is in accordance with the observation that pitch (the last state) is the integral of pitch rate, and therefore no modeling uncertainty is present. Once the matrix M from (48) has been obtained, the observer gains G_l and G_n and the reconstruction weighting matrix W can be synthesized using the LMI optimization proposed in [19]. The choice of the filter matrix A_f impacts on the performance of the system. If the absolute value of the eigenvalues of A_f are small, then the bandwidth of the filtering properties is decreased. Consequently, during sliding, although the output of the observer may track the filtered outputs of the plant perfectly, the outputs of the observer no longer necessarily track the true output of the plant as accurately—consequently, there is a reduction in performance in terms of the state estimation properties. Conversely, large negative eigenvalues for A_f improve the state estimation performance. However, the state estimation performance is not the key criteria here. More importantly, the choice of A_f affects the optimal value of $\hat{\gamma} = \|\hat{G}(s)\|_\infty$. Often, if the bandwidth of the filter associated with A_f is lower than the natural frequency of any oscillatory modes in the plant, then the optimal value of $\hat{\gamma}$ which is obtained from the LMIs may be reduced/improved, and consequently smaller eigenvalues for A_f maybe preferable. Therefore, the selection of A_f is a crucial part of the initial design iteration. Here, A_f from (47) has been chosen as $A_f = 0.01 \times I_4$. Assume that the pitch rate q, true air speed V_{tas}, and angle of attack α measurements are fault-free, and therefore N_p from (45) is defined as $N_p^T = [0\ 0\ 0\ 1]$ Using the fault reconstruction method based on the observer described in Section IV-A applied to the augmented system, and choosing $D_1 = \text{diag}(0.1\ 0.11\ 0.1\ 0.1)$ and $\hat{\gamma}_o = 0.003$, a value of $\|\hat{G}(s)\|_\infty = 5.8668 \times 10^{-4}$ has been obtained from the LMI optimization. The choice of the design matrix D_1 has been used to fine tune the observer gain G_l, while $\hat{\gamma}_o$ is chosen to be small to ensure that the $\mathcal{H}_\infty$ norm of $\hat{G}(s)$ from (54) is small (which means that the fault reconstruction will be less affected by the uncertainty). When trying to ensure that the $\mathcal{H}_\infty$ norm of $\hat{G}(s)$

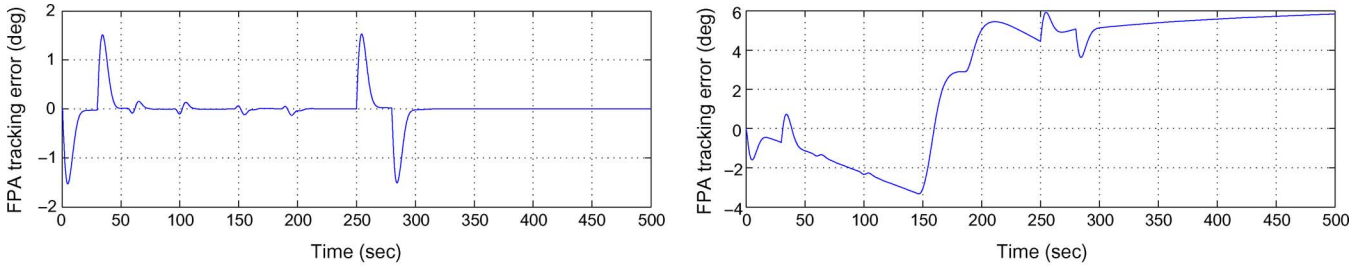

Fig. 4. Fault simulation: FPA tracking error: fault —free and with fault (FDI switched off). (a) Fault-free. (b) Fault on the θ sensor.

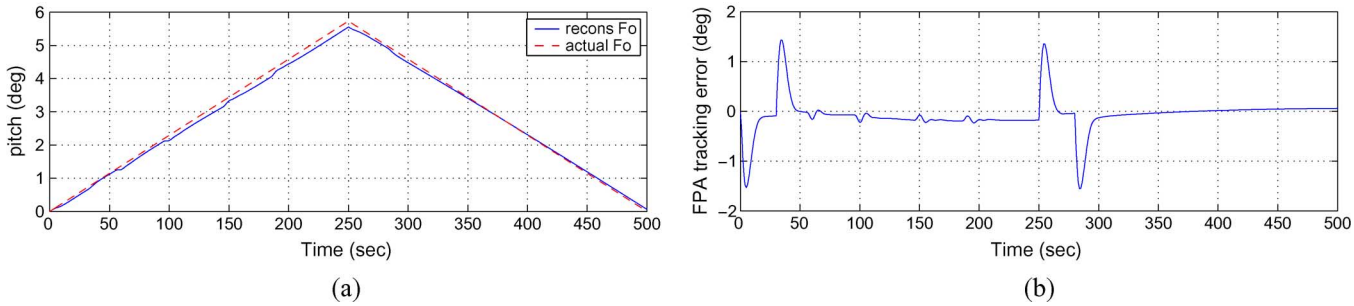

Fig. 5. Fault simulation responses: FDI switched on (without trim values). (a) Reconstructed fault. (b) FPA tracking error.

is small (using a small $\hat{\gamma}_o$), the observer gain G_l might become large and unrealistic for implementation. Therefore, in terms of design, there is a tradeoff between obtaining a small $\hat{\gamma}$ and a realistic observer gain G_l. The simulation parameters from (52) were chosen as $\rho_o = 50$ and $\delta_o = 0.005$. A large ρ_o is required to ensure that sliding still occurs in the presence of uncertainty and faults, and a small δ_o is necessary to closely approximate the discontinuous switching injection. The $\nu_{\rm eq}$ signal used for the reconstruction is filtered using a first-order low-pass filter with time constant 0.1 before being scaled by the weighting matrix W. This filtering operation is quite in keeping with the notion of the equivalent injection being the low-frequency component of ν [20]. In the same way, other observers can be designed to specifically reconstruct faults on the angle of attack and pitch rate measurement signals (although, as shown in [1], a fault on the pitch rate measurement does not significantly affect the closed-loop performance). A bank of observers [3] could then be employed to give fault tolerance to a range of sensor faults [1].

1) Sensor FTC Simulation Results: The effect of feeding the faulty sensor signals into the controller has been investigated. For comparison purposes, the performance of the scheme in Fig. 3 has been measured using the root mean square (RMS) of the FPA tracking error. As in Section III-B1, the same flight conditions and controller have been used. *Note that the simulations are done on the full 77 state nonlinear model of the B747-100/200*. The results presented in the following figures do not include the trim values for ease of interpretation. The fault signal was set as a sensor drift represented by a positive ramp signal starting from zero at the beginning of the simulation, with a peak of 5.73° at 250 s and then a negative ramp back to zero at 500 s [as in Fig. 5(a)]. Since the design assumes that the measurement for $V_{\rm tas}$ is free from faults, only the FPA tracking error is shown. When no fault occurs, the RMS of the error signal is 0.0150 [see Fig. 4(a)], but when a pitch sensor fault occurs and no compensation using $\hat{f}_o$ is employed, the RMS value becomes 0.1969 [see Fig. 4(b)]. Fig. 5 shows the case when the corrupted plant output signal is corrected by the fault reconstruction signal before being used by the controller, and therefore it is able to maintain performance. The FPA tracking error RMS value for Fig. 5(b) is 0.0154 (which is close to the RMS when there is no fault).

V. Conclusion

This paper has presented a sliding mode control scheme for fault tolerant control of a civil aircraft. As in the work of [6], only longitudinal control with a fault and/or failure occurring in the elevator channel has been considered. The controller is based around a state-feedback sliding-mode scheme, and the gain associated with the nonlinear term is allowed to adaptively increase when the onset of a fault is detected. Compared with other FTC schemes which have been implemented on this model, the controller proposed here is simple and yet is shown to work across the entire "up and away" flight envelope. It is not scheduled across any variables, and its structure remains fixed (except for the adaptive gain associated with the nonlinear switching term). Unexpected deviation of the switching variable from its nominal condition initiates the adaptation mechanism. Total failure can also be detected from the switching function and in this example has been used to trigger the use of a "backup" control surface. A range of realistic fault scenarios have been considered, and the results of simulations using the full nonlinear aircraft model have been presented. A sensor FTC scheme using the same controller is also proposed. The scheme is based on the reconstruction of sensor faults using a sliding-mode observer. The fault reconstructions are then used to correct the measured outputs before being used in the controller calculations, and therefore the controller does not need to be reconfigured.

REFERENCES

[1] H. Alwi and C. Edwards, "Robust sensor fault estimation for tolerant control of a civil aircraft using sliding modes," in *Proc. Silver Anniv. Amer. Control Conf.*, 2006, pp. 5704–5709.

[2] S. P. Boyd, L. El Ghaoui, E. Feron, and V. Balakrishnan, *Linear Matrix Inequalities in Systems and Control Theory*. Philadelphia, PA: SIAM, 1994.

[3] J. Chen and R. J. Patton, *Robust Model-Based Fault Diagnosis for Dynamic Systems*. Boston, MA: Kluwer, 1999.

[4] C. Edwards and S. K. Spurgeon, *Sliding Mode Control: Theory and Applications*. New York: Taylor & Francis, 1998.

[5] C. Edwards, S. K. Spurgeon, and R. J. Patton, "Sliding mode observers for fault detection," *Automatica*, vol. 36, pp. 541–553, 2000.

[6] S. Ganguli, A. Marcos, and G. J. Balas, "Reconfigurable LPV control design for Boeing 747-100/200 longitudinal axis," in *Proc. Amer. Control Conf.*, 2002, pp. 3612–3617.

[7] C. Hanke and D. Nordwall, The Simulation of a Jumbo Jet Transport Aircraft. Volume II: Modelling Data NASA and The Boeing Company, Technical Report CR-114494/D6-30643-VOL2, 1970.

[8] R. A. Hess and S. R. Wells, "Sliding mode control applied to reconfigurable flight control design," *J. Guid., Control Dynam.*, vol. 26, pp. 452–462, 2003.

[9] M. Huzmezan and J. Maciejowski, Reconfigurable Flight Control Methods and Related Issues—A Survey Univ. of Cambridge, 1997, Technical report prepared for the DERA under the research agreement no. ASF/3455.

[10] H. K. Khalil, *Nonlinear Systems*. Englewood Cliffs, NJ: Prentice-Hall, 1992.

[11] J. M. Maciejowski and C. N. Jones, "MPC fault-tolerant control case study: Flight 1862," in *Proc. IFAC Symp. SAFEPROCESS*, 2003, pp. 121–125.

[12] A. Marcos and G. J. Balas, A Boeing 747-100/200 Aircraft Fault Tolerant and Diagnostic Benchmark Dept. of Aerosp. Eng. Mech., Univ. of Minnesota, Tech. Rep. AEM-UoM-2003-1, 2003.

[13] A. Marcos and G. J. Balas, "A robust integrated controller/diagnosis aircraft application," *Int. J. Robust and Nonlinear Control*, vol. 15, pp. 531–551, 2005.

[14] A. Marcos, S. Ganguli, and G. J. Balas, "An application of H_∞ fault detection and isolation to a transport aircraft," *Control Eng. Practice*, vol. 13, pp. 105–119, 2005.

[15] R. J. Patton, "Robustness in model-based fault diagnosis: The 1997 situation," *IFAC Ann. Rev.*, vol. 21, pp. 101–121, 1997.

[16] Y. Shtessel, J. Buffington, and S. Banda, "Tailless aircraft flight control using multiple time scale re-configurable sliding modes," *IEEE Trans. Control Syst. Technol.*, vol. 10, no. 3, pp. 288–296, May 2002.

[17] M. H. Smaili, Flightlab 747: Benchmark for Advance Flight Control Engineering Tech. Univ. Delft, Delft, The Netherlands, 1999, Tech. Rep..

[18] C. P. Tan and C. Edwards, "Sliding mode observers for detection and reconstruction of sensor faults," *Automatica*, pp. 1815–1821, 2002.

[19] C. P. Tan and C. Edwards, "Sliding mode observers for robust detection and reconstruction of actuator and sensor faults," *Int. J. Robust Nonlinear Control*, vol. 13, pp. 443–463, 2003.

[20] V. I. Utkin, *Sliding Modes in Control Optimization*. Berlin, Germany: Springer-Verlag, 1992.

[21] C. A. A. M. van der Linden, DASMAT: Delft University Aircraft Simulation Model and Analysis Tool Tech. Univ. Delft, Delft, The Netherlands, Tech. Rep. LR-781, 1996.

[22] G. Wheeler, C. Su, and Y. Stepanenko, "Sliding mode controller with improved adaptation laws for the upper bounds on the norm of uncertainties," *Automatica*, vol. 34, pp. 1657–1661, 1998.

[23] J. X. Xu, Q. W. Jia, and T. H. Lee, "On the design of a nonlinear adaptive variable structure derivative estimator," *IEEE Trans. Autom. Control*, vol. 45, no. 8, pp. 1028–1033, Aug. 2000.

[24] Y. Zhang and J. Jiang, "Bibliographical review on reconfigurable fault tolerant control systems," in *Proc. IFAC Symp.*, Washington, DC, 2003, pp. 265–276.

[25] K. Zhou, J. C. Doyle, and K. Glover, *Robust and Optimal Control*. Upper Saddle River, NJ: Prentice-Hall, 1996.